Impact-Parameter Dependence of Ar^+-Induced Kinetic Electron Emission from Ni{110}

J. W. Rabalais, H. Bu, and C. D. Roux
Department of Chemistry, University of Houston, Houston, Texas 77204-5641
(Received 4 November 1991; revised manuscript received 12 May 1992)

Electron intensities resulting from 4-keV Ar^+ impingent on Ni{110}-$p(1\times1)$ and Ni{110}-$p(1\times2)$-H surfaces exhibit sharp azimuthal- (δ) and incident- (α) angle anisotropies. The electron and scattered-Ar δ distributions are similar, indicating that electrons are emitted only from collisions whose impact parameters (p) are less than a threshold value (p_{max}). Comparison of the α-angle variations of the electrons and scattered Ar shows that the distance of closest approach corresponding to p_{max} is ≈ 0.3 Å. This corresponds to the sum of the radii of maximum radial charge density of the L atomic shells of Ar and Ni.

PACS numbers: 61.80.Jh, 52.20.Hv, 52.25.Tx, 79.20.Nc

Ions impinging on a surface can stimulate electron emission by means of two distinguishable mechanisms, potential [1] and kinetic [2] emission. In potential emission, potential energy released upon neutralization of the ion provides energy for ejection of electrons. This mechanism has no kinetic energy threshold and is spontaneous if the neutralization energy of the ion is greater than twice the work function of the solid. In kinetic emission, energy for ejection of electrons is supplied by the kinetic energy of the ion. During a collision, kinetic energy is transferred to both the nucleus and the electrons of the target atom. The nucleus recoils and the electrons are excited. Electronic excitation is produced by the mutual repulsion of overlapping electronic shells. Kinetic emission becomes relatively more important than potential emission at ion velocities $\gtrsim 10^7$ cm/s.

Much data have been acquired [2–7] on ion-induced kinetic electron emission, but, although theories have been proposed, mechanistic details are poorly understood (see Refs. [8–13] for reviews). These theoretical treatments range from direct excitation of target electrons in the hard collision to excitation resulting from Auger decay of inner-shell vacancies. The influence of the ordered structure of the target on kinetic emission has been studied [8] for ion energies $\gtrsim 10$ keV and high incident angles. Under these conditions, ions penetrate into the target and directional effects are controlled by the bulk crystal structure and channeling. The impact-parameter (p) dependence and the influence of the surface crystal structure on the electron emission process are not known.

This paper correlates the surface-structure sensitivity of the intensities of scattered atoms and emitted secondary electrons in order to determine the distance of closest approach required for stimulation of kinetic electron emission. The systems of 4-keV Ar^+ scattering from a clean Ni{110}-$p(1\times1)$ surface and a hydrogen-covered Ni{110}-$p(1\times2)$-H missing-row-reconstructed [14] surface provide examples. To the best of our knowledge, this is the first measurement of the threshold impact-parameter dependence of kinetic emission. This has important implications in the theory of kinetic emission and in developing a charge-transfer microscopy.

Measurements were carried out in a time-of-flight scattering and recoiling spectrometer (TOF-SARS) which has been described elsewhere [15]. Briefly, a monoenergetic, pulsed, rare-gas ion beam is directed onto a sample. The scattered and recoiled neutrals and ions along with the emitted electrons are velocity analyzed along a 0.93-m flight path and detected by a channel electron multiplier. Spectra are collected in a multichannel pulse height analyzer. The experimental parameters employed were a 4-keV pulsed Ar^+ beam, a pulse width of ≈ 30 ns, a pulse rate of ≈ 30 kHz, and current density < 0.1 nA/mm^2.

The Ni sample was a 10-mm disk with a polished {110} face which was cleaned by 3-keV Ar^+ bombardment and 800-K annealing cycles. The absence of H, C, and O recoils in the TOF-SARS confirmed the surface cleanliness. The clean $p(1\times1)$ surface was obtained by flashing to 800 K and the $p(1\times2)$-H surface was obtained by introducing 3×10^{-7} torr of H_2 while the sample cooled down from its annealing temperature.

A representative TOF spectrum is shown in Fig. 1 for the clean Ni{110} surface. It consists of peaks due to scattered and recoiled particles as well as emitted electrons. The electron peak is at $t \approx 0$ on the μs scale and indicates the origin of the time scale. It was ascertained that this peak is due to electrons and not photons by electrostatic deflection of the particles along the flight path. Identification of scattered and recoiled particles is obtained through kinematic relations [16,17]. The intensities of the scattering $I_{(S)}$ and electron $I_{(e)}$ signals are determined by integrating a narrow window centered on the TOF peaks.

The electron energy spectrum was measured by scanning a hemispherical electrostatic analyzer situated at an angle of 75° from the incident ion beam. The energy spectrum exhibited a smooth distribution which peaked at < 5 eV and extended to ≈ 25 eV as shown previously [2] for similar systems. No narrow peaks characteristic of autoionization or Auger processes were observed [18]. This spectrum is typical of electron distributions induced

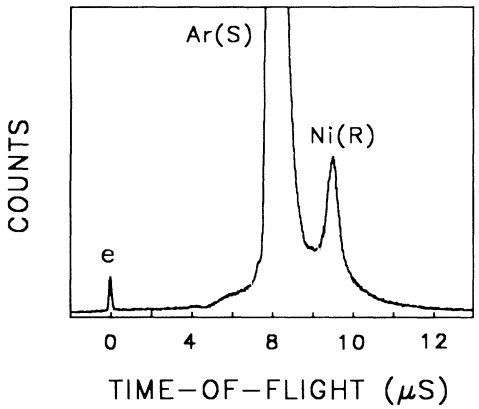

FIG. 1. TOF spectrum of scattered neutrals+ions [Ar(S)], recoiled nickel [Ni(R)], and collision-induced electron emission (e) for 4-keV Ar^+ scattering from a Ni{110}-$p(1\times1)$ surface. Scattering angle $\Theta=35°$, incident angle $\alpha=10°$, and azimuthal angle $\delta=65°$.

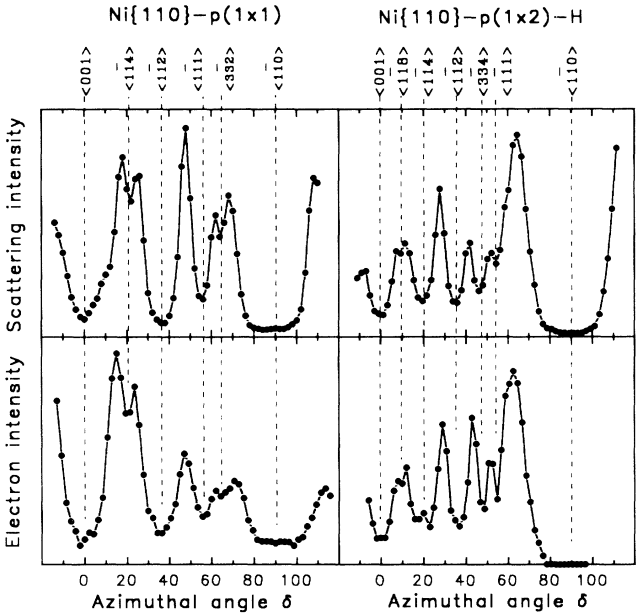

FIG. 2. Scattering intensity $I_{(S)}$ and electron intensity $I_{(e)}$ vs azimuthal angle δ for 4-keV Ar^+ scattering from a Ni{110}-$p(1\times1)$ and a Ni{110}-$p(1\times2)$-H missing-row-reconstructed surface. The scattering angle $\Theta=35°$ and the incident angle $\alpha=8°$. $\delta=0°$ and 90° correspond to the $\langle001\rangle$ and $\langle1\bar{1}0\rangle$ azimuths, respectively.

by kinetic energy transfer from the projectile.

As has been demonstrated [19], the scattering intensity $I_{(S)}$ is modulated by the first-layer azimuthal structure when measured at glancing incident angle α. Such $I_{(S)}$ vs δ patterns are shown in Fig. 2 for the (1×1) and (1×2)-H surfaces. Minima are observed along low-index azimuths because the scattering centers are inside of the shadow cones cast by the aligned nearest neighbors. As δ is scanned, the scattering centers move out of the shadow cones along intermediate δ directions where atoms are not aligned and a resulting increase in $I_{(S)}$ is observed. These minima reveal [19] the directions along which first-layer nearest neighbors exist.

The electron intensity $I_{(e)}$ vs δ scans in Fig. 2 show that the electron yield pattern is analogous to that of the scattered atoms. These results indicate that electron emission is produced by small-p collisions which are accessible along intermediate azimuths. Along low-index azimuths where atoms are aligned, only large-p collisions are possible at glancing α due to shadowing.

Examples of $I_{(S)}$ and $I_{(e)}$ vs α scans along the $\langle1\bar{1}0\rangle$ azimuth are shown in Fig. 3. As α is increased along low-index azimuths, first-layer atoms move out of the shadow cones of their first-layer neighbors. When the p value required for scattering into the detection angle is attained, a sharp increase in $I_{(S)}$ is observed. Measurement of this scattering critical angle $\alpha_{(S),c}$ allows calculation [20] of the interatomic spacing (d), if the shadow-cone radius (R) is known, or it provides a calibration for R if d is known. The $I_{(e)}$ vs α scans exhibit similar features which define an electron emission critical angle $\alpha_{(e),c}$.

The maximum value of p capable of producing kinetic emission, $p_{\max}$, can be determined from $\alpha_{(S),c}$ and $\alpha_{(e),c}$ if the shadow-cone shape is known. The dependence of the shadow-cone radius $R(L)$ on the distance L behind the shadowing atom was calculated using the Moliére potential and the binary collision approximation [20]. A calibrated shadow cone [20] was obtained by adjusting the screening constant of the potential to a value of $C=0.68$ in order to fit the experimental shadow-cone parameters obtained for Ne scattering from clean Ni. This calibrated potential was used to calculate p for scattering into specific angles and the distance of closest approach (R_c) of the colliding nuclei.

Consider the case of $I_{(S)}$ vs α in Fig. 3. Along the $\langle1\bar{1}0\rangle$ azimuth the interatomic spacing is $d=2.49$ Å. For 4-keV Ar scattering from Ni into a scattering angle of $\Theta=45°$, $p=0.23$ Å and $R_c=0.37$ Å. The measurement in Fig. 3 yields $\alpha_{(S),c}=15.3°$; hence the cone radius is $R=d\sin\alpha_{(S),c}+p=0.89$ Å at a distance behind the target atom of $L=d\cos\alpha_{(S),c}=2.40$ Å. This R value can be compared to that obtained from the shadow cone, i.e., $R=0.91$ Å at $L=2.40$ Å, which differs from the experimental value by only 2%.

Now consider the case of $I_{(e)}$ vs α in Fig. 3. The result that $\alpha_{(e),c}>\alpha_{(S),c}$ indicates that the p required for electron emission in the collision is smaller than that required for scattering of Ar into $\Theta=45°$. The measurement yields $\alpha_{(e),c}=18.4°$; thus $r=d\sin\alpha_{(e),c}=0.79$ Å and $L=d\cos\alpha_{(e),c}=2.36$ Å. Since the radii of the cones R at $L=2.40$ and 3.26 Å are similar (they differ by 0.003 Å), the maximum p for electron emission in the collision is then given by $p_{\max}=R-r=0.10$ Å; this corresponds to $R_c=0.30$ Å.

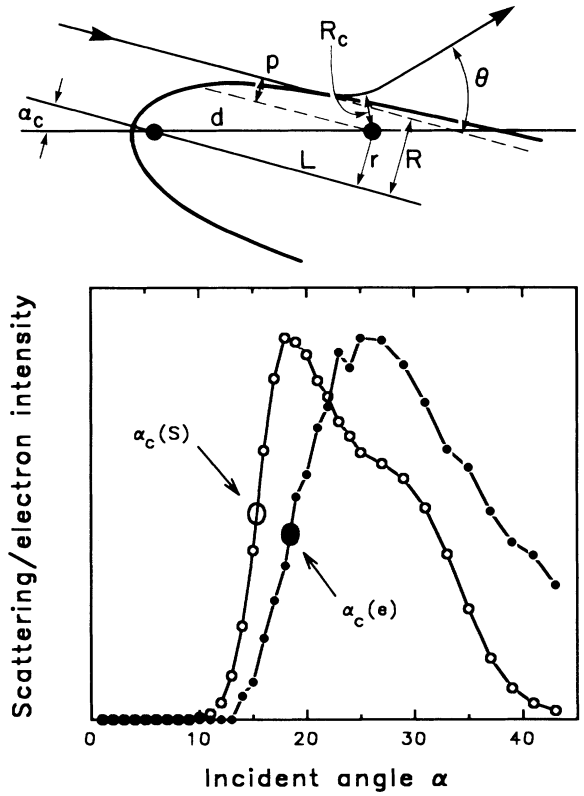

FIG. 3. Scattering intensity $I_{(S)}$ and electron intensity $I_{(e)}$ vs incident angle α along the $\langle 1\bar{1}0\rangle$ azimuth ($\delta=90°$) for the Ni{110}-$p(1\times2)$ surface using a scattering angle of $\Theta=45°$. The schematic illustrates the relationship between the shadow cone, impact parameter, and incident angle.

A p value of 0.1 Å produces scattered Ar at $\Theta\approx90°$. Kinetic emission, therefore, results from collisions for which Ar is single scattered at an angle $\Theta\geq90°$. Secondary electrons can be measured with the detector at $\Theta=45°$, or at any angle, since they have an angular distribution [8–11] which is approximately $1/\sin\beta$ (where β is the electron ejection angle from the surface). This results from the fact that the electron emission angle is independent of the p giving rise to the emission. This differs from the case of scattered atoms, where placement of the detector at a specific scattering angle Θ results in detection of only those atoms that have scattered with a specific $p(\Theta)$ value.

These considerations are confirmed by two types of measurements. (1) For α scans at fixed scattering angle Θ and different azimuthal angles δ, both $\alpha_{(e),c}$ and $\alpha_{(S),c}$ increase with decreasing interatomic spacing along the azimuth. This shows that *electron emission is stimulated by incoming trajectories with* $p\leq p_{\max}$, since small-p collisions are possible only at high α along close-packed azimuths. (2) For α scans along a fixed azimuth δ and different scattering angles Θ, $\alpha_{(e),c}$ is constant (within an experimental error of $\pm0.3°$) and $\alpha_{(S),c}$ increases with Θ as $\alpha_{(S),c}=14.8°$, 15.1°, 15.3°, and 16.0° for $\Theta=35°$, 40°, 45°, and 51°, respectively. Using the decrease in p with increasing Θ, the corresponding calculated $\alpha_{(S),c}$ values are 14.4°, 15.1°, 15.6°, and 16.3°, in good agreement with observed values. As Θ increases, $\alpha_{(S),c}$ approaches $\alpha_{(e),c}$ and eventually the $I_{(S)}$ vs α and $I_{(e)}$ vs α curves should coincide at $\Theta=90°$. We cannot obtain these data because for $\Theta\gtrsim70°$, neutral Ar (> 99% of the scattered flux is neutral) has too low a velocity to be detected by the electron multiplier and also for $\Theta\gtrsim52°$ there is considerable multiply scattered Ar which obscures the intensity measurement of the weakening single-scattered Ar peak. Nevertheless, the result that $\alpha_{(S),c}$ approaches the constant $\alpha_{(e),c}$ as Θ increases indicates that *the electron emission angle is independent of* p *for* $p\leq p_{\max}$.

The maximum R_c determined above for electron emission provides insight into the collisional electron promotion mechanism. Electronic excitation and ionization in keV collisions are due to inelastic processes which are often observed as emission of electrons or photons, variations in the type and abundance of specific charge states of scattered species, and displacements in the energy and angle of the scattered particles from the elastic position. The current understanding of these processes is based on evolution of molecular orbitals (MO's) of the quasi dimolecule formed during the close collision. Fano and Lichten [21,22] have described such electron promotion in the quasidiatomic molecule. As interatomic distance decreases, MO's evolve from atomic orbitals (AO's) of the separate atoms of atomic number Z_1 and Z_2 into the AO of the "united atom" of atomic number Z_1+Z_2. This evolution of MO's is dominated by (i) a reduced binding energy at short distances due to repulsion between electrons and (ii) the availability of electronic states as constrained by the Pauli principle and symmetry rules. Electronic excitations in such encounters can be predicted from separated-atom–united-atom diagrams with diabatic correlations [23]. Electrons can be promoted from filled AO's into weakly bound MO's from which they are trapped in higher-principal-quantum-number AO's as the atoms recede. Some of these AO's correspond to continuum states of the individual atoms, resulting in electron emission.

It has been shown [24–26] that inelastic energy losses in gas-phase collisions are directly dependent on R_c. For Ne^+-Ne and Ar^+-Ar collisions, a sharp increase in the inelastic energy loss, number of ejected electrons, and number of excited atoms occurs at collision energies for which there is significant overlap of the L atomic shells of the colliding pair [21]. The sum of the radii of maximum radial charge density (r) for the electronic subshells of the Ar-Ni pair is as follows [27]: 1s, 0.05 Å; 2s, 0.31 Å; 2p, 0.25 Å; and 3s,3p, $\approx$1.01 Å. The maximum R_c value of 0.30 Å determined here for kinetic emission is close to r for the $L(2s,2p)$ shells of the colliding pair. Since this R_c value is outside of the overlap region of the core $K(1s)$ shells and 3 times smaller than the overlap re-

gion of the valence $M(3s,3p)$ shells, it is apparent that the critical internuclear distance for electron emission corresponds to overlap of the L shells. It is noted that previous work by Ferron *et al.* [28] also suggested a p dependence of collisional-induced electron emission, i.e., emission occurs when a p value is attained such that the transferred energy exceeds the surface work function.

In summary, our results show the following: (i) Kinetic electron emission exhibits a threshold impact-parameter dependence, with emission occurring only for $p \leq p_{\max}$. (ii) The critical incident angles for ion scattering and electron emission can be used to calculate the distance of closest approach required for kinetic emission of electrons. This distance is $R_c \approx 0.3$ Å, corresponding to overlap of the Ar and Ni L subshells. (iii) The intensity of kinetic emission stimulated by low-energy ions exhibits sharp azimuthal anisotropy which is determined by the structure of the outermost atomic layer. These results are consistent with a kinetic electron emission mechanism which requires a specific overlap of inner electron subshells, resulting in promotion of electrons into excited levels from which they are spontaneously emitted.

This material is based on work supported by the National Science Foundation under Grant No. DMR-8914608 and the R. A. Welch Foundation under Grant No. E-656. C.D.R. gratefully acknowledges support from an IBM Graduate Fellowship award.

[1] H. D. Hagstrum, in *Electron and Ion Spectroscopy of Solids*, edited by L. Fiermans, J. Vennik, and W. Dekeyser (Plenum, New York, 1978).
[2] D. E. Harrison, Jr., C. E. Carlston, and G. D. Magnuson, Phys. Rev. **139**, A737 (1965).
[3] U. Von Gemmingen, Surf. Sci. **120**, 334 (1982).
[4] R. A. Baragiola, E. V. Alonso, J. Ferron, and A. Oliva-Florio, Surf. Sci. **90**, 240 (1979); J. Ferron, E. V. Alonso, R. A. Baragiola, and A. Oliva-Florio, J. Phys. D **14**, 1707 (1981).
[5] K. O. Ohya, J. Kawata, and I. Mori, Jpn. J. Appl. Phys. **28**, 1944 (1989).
[6] T. Kanie, K. Oda, A. Ichimiya, T. Yasue, S. Ohtani, and H. Tawara, Surf. Sci. **242**, 417 (1991).
[7] S. T. De Zwart, A. G. Drentje, A. L. Boers, and R. Morgenstern, Surf. Sci. **217**, 298 (1989).
[8] B. A. Brusilovsky, Vacuum **35**, 595 (1985).
[9] S. Y. Lai, D. Briggs, A. Brown, and J. C. Vickerman, Surf. Interface Anal. **8**, 93 (1986).
[10] J. Los and J. J. C. Geerlings, Phys. Rep. **190**, 133 (1990).
[11] R. Brako and D. M. Newns, Rep. Prog. Phys. **52**, 655 (1989).
[12] P. Varga and H. Winter, in *Particle Induced Electron Emission II*, Springer Tracts in Modern Physics Vol. 123 (Springer, Berlin, 1992), p. 149.
[13] W. O. Hofer, Scanning Micro. Suppl. **4**, 265 (1990).
[14] C. Roux, H. Bu, and J. W. Rabalais, Surf. Sci. (to be published).
[15] O. Grizzi, M. Shi, H. Bu, and J. W. Rabalais, Rev. Sci. Instrum. **61**, 740 (1990).
[16] J. W. Rabalais, CRC Crit. Rev. Solid State Mat. Sci. **14**, 319 (1988).
[17] J. W. Rabalais, Science **250**, 521 (1990).
[18] P. A. A. F. Wouters, P. A. Zeijlmans Van Emmichoven, and A. Niehaus, Surf. Sci. **211/212**, 249 (1989).
[19] F. Masson, H. Bu, M. Shi, and J. W. Rabalais, Surf. Sci. **249**, 313 (1991).
[20] O. Grizzi, M. Shi, H. Bu, J. W. Rabalais, and P. Hochmann, Phys. Rev. B **40**, 10127 (1989).
[21] W. Lichten, J. Phys. Chem. **84**, 2102 (1980).
[22] U. Fano and W. Lichten, Phys. Rev. Lett. **14**, 627 (1965).
[23] F. T. Smith, Phys. Rev. **179**, 111 (1969).
[24] J. C. Brenot, D. Dhuicq, J. P. Gauyacq, J. Pommier, V. Sidis, M. Barat, and E. Pollack, Phys. Rev. A **11**, 1245 (1975).
[25] M. Barat and W. Lichten, Phys. Rev. A **6**, 211 (1972).
[26] B. Fastrup, G. Hermann, and K. J. Smith, Phys. Rev. A **3**, 1591 (1971).
[27] J. C. Slater, *Quantum Theory of Atomic Structure* (McGraw-Hill, New York, 1960), Vol. I.
[28] J. Ferron, E. V. Alonso, R. A. Baragiola, and A. Oliva-Florio, J. Phys. D **14**, 1707 (1981).